THE JOURNAL OF PHYSICAL CHEMISTRY A

Article

pubs.acs.org/JPCA

Thermal Decomposition Mechanism for Ethanethiol

AnGayle K. Vasiliou,*[,†] Daniel E. Anderson,[†] Thomas W. Cowell,[†] Jessica Kong,[‡,†] William F. Melhado,[†] Margaret D. Phillips,[†] and Jared C. Whitman[†]

[†]Department of Chemistry and Biochemistry, Middlebury College, Middlebury, Vermont 05753, United States

ABSTRACT: The thermal decomposition of ethanethiol was studied using a 1 mm × 2 cm pulsed silicon carbide microtubular reactor, $CH_3CH_2SH + \Delta \rightarrow$ Products. Unlike previous studies these experiments were able to identify the initial ethanethiol decomposition products. Ethanethiol was entrained in either an Ar or a He carrier gas, passed through a heated (300−1700 K) SiC microtubular reactor (roughly ≤100 μs residence time) and exited into a vacuum chamber. Within one reactor diameter the gas cools to less than 50 K rotationally, and all reactions cease. The resultant molecular beam was probed by photoionization mass spectroscopy and IR spectroscopy. Ethanethiol was found to undergo unimolecular decomposition by three pathways: $CH_3CH_2SH \rightarrow$ (1) $CH_3CH_2 + SH$, (2) $CH_3 + H_2C{=}S$, and (3) $H_2C{=}CH_2 + H_2S$. The experimental findings are in good agreement with electronic structure calculations.

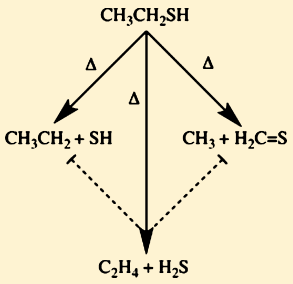

1. INTRODUCTION

Raw energy sources including coal, petroleum, and biomass contain varying quantities of sulfur contaminants. Converting raw energy sources into usable liquid fuels is a complicated process involving many steps, but two aspects are common to all methods: (1) the use of heat to break chemical bonds of larger organic molecules into smaller semivolatile or volatile species and (2) the need to remove sulfur during the refining process. The thermolysis chemistry of the sulfur compounds encountered in petroleum and biofuels is poorly understood and, in some cases, completely unknown. The current foundations in this field are based on end point chemistry, meaning that the reaction mechanisms have been proposed without direct evidence of radical intermediates. This knowledge gap hinders any progress in refinery cleanup methodology, as current efforts for improving sulfur removal technologies are done with an incomplete picture of the molecular level chemistry.

Despite the importance of sulfur in industrial processing, there has been very little attention to the pyrolysis of organic sulfur compounds. The thermal chemistry of ethanethiol has been studied sporadically over the years, which has resulted in several proposed thermal decomposition mechanisms.[1−4] Previous work focused on the disappearance of the parent thiol with little attention, as a result of experimental limitations, to the identification and characterization of thermal decomposition products. The lack of experimental information on initial decomposition products has led to disagreement on the reaction mechanisms for ethanethiol and many other alkanethiols.[5−9]

Sehon et al.[2] and Bamkole et al.[5] proposed a radical mechanism for ethanethiol pyrolysis initiated by the cleavage of the C−S bond. Sehon et al. also suggested a second possible mechanism along with Thompson et al. that proceeds by molecular elimination reactions.[8,9] Recent theoretical work by Baldridge et al.[10] predicts that the molecular elimination channels for alkanethiols are unfavorable at low temperatures (below 1000 K) as a result of the relatively high reaction barriers compared with that of the more energetically favored radical reaction pathway in which the C−S bond is cleaved. However, Baldrige et al. predicts that at higher temperatures (above 1000 K) the molecular elimination channels will be competitive with radical processes.[10]

The thermal pyrolysis of ethanethiol shown in (1) has been studied in static reactors, flow reactors, and flames over the last 80 years.[1−4]

$$CH_3CH_2SH + \Delta \rightarrow \text{Products} \quad (1)$$

Our present view on the thermal cracking of ethanethiol, CH_3CH_2SH, is based on the early analysis of Sehon et al.[2] who suggested two thermal decomposition channels. The lower temperature pathway (785−938 K) (2) proceeds by molecular rearrangement to form ethylene (C_2H_4) and hydrogen sulfide (H_2S)

$$CH_3CH_2SH \rightarrow C_2H_4 + H_2S \quad (2)$$

and, at high temperatures, by a free radical (1005−1102 K) mechanism (3) to form the ethyl radical (C_2H_5) and sulfanyl (or mercaptal) radical (SH).

$$CH_3CH_2SH \rightarrow C_2H_5 + SH \quad (3)$$

The compounds observed by Sehon et al. were H_2S, C_2H_4, H_2, and CH_4. Due to the experimental limitations of Sehon et al. as well as other previous studies, reactive intermediates (i.e., SH radical in (3)) produced as pyrolysis products were unable to be detected. For this reason, the current mechanism for the thermal decomposition of ethanethiol is based on end point chemistry without direct evidence of radical intermediates. As is the case with many molecules including ethanethiol, when end point chemistry alone is used to propose thermal decomposition, mechanisms often the most rich and unexpected chemistry is overlooked.

Received: March 20, 2017
Revised: May 20, 2017
Published: May 30, 2017

DOI: 10.1021/acs.jpca.7b02629
J. Phys. Chem. A 2017, 121, 4953−4960

To understand reaction 1, it is important to examine the thermochemistry of ethanethiol as this will provide a powerful basis for the initial unimolecular decomposition channels. The thermochemistry for ethanethiol is well-known.[11] The two weakest bonds in ethanethiol are the C−S bond,[12−14] $DH_{298K}(CH_3CH_2-SH)$ = 73.6 ± 0.5 kcal mol^{-1}, and the C−C bond,[13] $DH_{298K}(CH_3-CH_2SH)$ = 82.5 ± 2.2 kcal mol^{-1}. On the basis of thermochemistry, it is expected that unimolecular decomposition chemistry will be initiated by the cleavage of these two bonds.

In this study, the thermal decomposition of ethanethiol was investigated using a pulsed microtubular reactor and two different methods of detection. The products of the reaction were monitored using 118.2 nm (10.487 eV) vacuum ultraviolet photoionization mass spectrometry (PIMS) and matrix isolation IR spectroscopy. Within the microtubular reactor, ethanethiol seeded in an inert carrier gas is rapidly heated to 1000−1300 K, and decomposition is initiated. The relatively short residence time in the reactor (50−100 μs) ensures that the observed chemistry emphasizes the unimolecular processes excluding all but the most rapid bimolecular chemistry.

2. EXPERIMENTAL SECTION

A high-temperature pulsed microtubular reactor (or hyperthermal nozzle) was used to decompose ethanethiol. The microtubular reactor is a version of the Chen−Ellison reactor that has been used for several years to produce reactive intermediates.[15−26] The hyperthermal nozzle features a (1 mm i.d. × 3 cm long) SiC tube that can be heated up to 1700 K, with the temperature monitored by a type C thermocouple mounted to the outer wall of the SiC tube. A benefit of the microtubular reactor is the short residence time (50−100 μs).[27] This short residence time eliminates problems one might face in a typical vacuum pyrolysis experiment, including secondary reactions.[28−34]

Thermal cracking products are produced by pulsing ethanethiol, CH_3CH_2SH, seeded in an inert gas (roughly 1−2 atm) through the resistively heated SiC tube into a vacuum chamber. The valve can be fired at a nominal rate of 10−50 Hz. The ethanethiol/Ar (≤0.1%) mixture is injected into the SiC tube where it undergoes thermal decomposition and expands supersonically into a vacuum chamber (≤10^{-6} Torr). The rotational, vibrational, and translational temperatures drop rapidly within a few reactor diameters. The dynamics of the pyrolysis and gas transport in the reactor has been well characterized using computational fluid dynamics and will not be discussed here.[27] Two independent spectroscopic techniques, matrix isolation IR spectroscopy and PIMS, are used to monitor and characterize the output of the microreactor. Figure 1 provides a schematic of the experimental apparatus.

Matrix isolation infrared spectroscopy involves freezing the gas that is to be analyzed to a cold CsI window and then probing with infrared light. The microtubular reactor is mounted to the vacuum shroud of a Sumitumo CKW-21 two-stage closed-cycle helium cryostat. The nascent cracking products, seeded in Ar, that exit the reactor pass through a heat shield aperture plate and are deposited on a CsI window cooled to 5 K. The CsI window is approximately 2.5 cm from the exit of the reactor. The infrared spectrum was measured using a Thermo Scientific Nicolet iS50 FTIR with a mercury/cadmium/telluride (MCT-A) detector. IR spectra were collected within the frequency range 4000−500 cm^{-1}. The IR beam passes through a pair of CsI side windows attached to the Sumitumo vacuum shroud. A benefit to the matrix isolation apparatus is that it allows for accumulation of nascent thermal decomposition products over time, promoting good signal-to-noise, while simultaneously isolating the nascent products from each other within the matrix to prevent any secondary reactions.

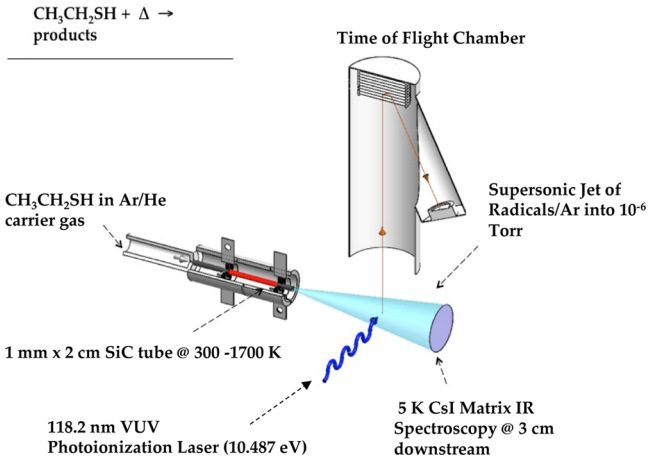

Figure 1. Schematic of the pulsed microtubular reactor used for ethanethiol thermal cracking. Samples were collected in a 5 K cryogenic matrix for analysis by infrared absorption spectroscopy or photoionized with fixed frequency vacuum ultraviolet (VUV) light with ion detection by a time-of-flight mass spectrometer.

The photoionization time-of-flight mass spectrometer that was used in these experiments has been described in more detail elsewhere; therefore, it is only briefly discussed here.[35,36] In contrast to the matrix isolation setup, as the nascent cracking products exit the microtubular reactor, the supersonic jet is skimmed approximately 3−5 mm after exiting the SiC tube and intersects with a 10.487 eV (118.2 nm) laser beam. The 10.49 eV light is generated by the frequency tripling of the third harmonic (356.6 nm, 30 mJ/pulse) of a Nd:YAG. The new ions are injected by a positively biased repeller plate into a reflection time-of-flight tube and accelerated into the drift zone by a strong electric field. At the end of the flight tube, the ions are reflected back down to the microchannel plate detector biased at negative voltage. The PIMS provides mass-to-charge (m/z) information that complements the vibrational frequencies obtained via the matrix isolation experiment. The PIMS, unlike the matrix experiment, does not require an accumulation of products for detection, and therefore, the time duration for an experiment is shorter. A typical matrix experiment can take up to 4 h for a single temperature, whereas the PIMS experiments can accomplish several temperatures in 1 h. For this reason, the PIMS was used for quick determination of the optimal temperature for the thermal decomposition of ethanethiol.

3. RESULTS: THERMAL DECOMPOSITION OF ETHANETHIOL

Scheme 1 depicts the three product channels for the unimolecular thermal decomposition of ethanethiol found in this work.

Figure 2 shows the PIMS spectra of the decomposition of ethanethiol in the high-temperature microtubular reactor. The bottom trace is the mass spectrum that results when ethanethiol seeded in helium (0.067% C_2H_6S in He) was pulsed through the microtubular reactor at room temperature (300 K). The ionization energy (IE) of ethanethiol is 9.2922 ± 0.0007 eV.[37] Photoionization with 118.2 nm (10.487 eV) VUV light produced

DOI: 10.1021/acs.jpca.7b02629
J. Phys. Chem. A 2017, 121, 4953−4960

Scheme 1. Unimolecular Pathways for the Thermal Decomposition of Ethanethiol

$CH_3CH_2SH \longrightarrow$ a) $CH_3CH_2 + SH$; b) $CH_3 + H_2C{=}S + H$; c) $H_2C{=}CH_2 + H_2S$

the parent ion, $C_2H_6S^+$, at m/z 62 and a $^{34}S_1$ isotopomer peak at m/z 64. The (64/62) isotope is calculated to be 4% for $C_2H_6S^+$, which is consistent with natural abundance. The PIMS spectra at 900 and 1100 K were the same as that at room temperature. When the reactor was heated to 1300 K, product ions at m/z 33 and 34 were observed, which arise from the ionization of the SH radical (IE = 10.4219 ± 0.0004 eV)[38] and H_2S (IE = 10.4607 ± 0.0026 eV).[39] Figure 3 shows the PIMS spectra that result when the reactor is heated to 1400 K. The bottom trace in Figure 3 is the room-temperature mass spectrum of ethanethiol. When the reactor was heated to 1400 K, product ions at m/z 33 and 34 increase from SH and H_2S and new features at m/z 15, 28, and 46 are detected. The product ion at m/z 15 arises from the ionization of the methyl radical, CH_3 (IE = 9.843 ± 0.002 eV),[40] and at m/z 28 from the ionization of ethylene (IE = 10.5138 ± 0.0006 eV).[41] The product ion at m/z 46 arises from the ionization of thioformaldehyde, H_2CS (IE = 9.376 ± 0.003 eV).[42] Although the literature value for the ionization of ethylene (C_2H_2) is greater than our 10.487 eV laser pulse, careful studies of the photoionization efficiency curve show that $C_2H_4^+$ can appear around 10.47 eV.[41]

The PIMS in Figures 2 and 3 are very informative but only confirm the identity of molecular products by m/z. The matrix IR spectra shown in Figures 4−7 confirm the identity of thioformaldehyde (m/z 46), hydrogen sulfide (m/z 34), sulfanyl radical (m/z 33), and ethylene (m/z 28). Matrix IR spectra were collected for ethanethiol decomposition using the microtubular reactor. In Figures 4−7, the blue trace is a background scan of Ar at 300 K and the black trace is a background scan of 0.01% mixture of CH_3CH_2SH/Ar at 300 K.

The 1300 K matrix IR spectra shown in Figure 4 affirm the presence of thioformaldehyde, CH_2S, with IR transitions at 1055, 988, and 982 cm^{-1}. These bands closely match those previously reported in Ar matrices by Jacox et al.[43] and Torres et al.[44] An IR transition at 3025 cm^{-1} for ν_1 was also observed.[43,44] Figure 5 shows the IR spectrum of ethanethiol at 1300 K, which shows the production of the SH radical at 2595 cm^{-1} as a pyrolysis product. The IR band observed in this work compares well with the reported value of 2594 cm^{-1} in a matrix by Isoniemei et al.[45] The small peak at 2605 cm^{-1} was also observed by Isoniemei et al. and is likely attributed to the fact that the SH radical was undergoing rotation in the matrix. Although the majority of molecules do not rotate in the matrix environment, it is well-known that small molecules or radicals can undergo nearly unhindered rotation in the matrix.[46−49]

Figure 6 confirms the presence of ethylene, C_2H_4, as a product of ethanethiol decomposition. Figure 6 shows a comparison of the matrix IR spectrum of CH_3CH_2SH heated to 1300 K with that of a sample of pure ethylene that was deposited at room temperature. Figure 6 shows distinctive bands for ethylene in the wavelength ranges 1450−1410 and 1000−900 cm^{-1}. The IR bands at 1439 and 947 cm^{-1} in Figure 6 belong to ν_{12} and ν_7 of ethylene. In addition to ν_{12} and ν_7, vibrational modes ν_{11} = 2995 cm^{-1} and ν_9 = 3081 cm^{-1} were observed for ethylene. The IR spectra in Figure 7 confirm the presence of H_2S as a product from ethanethiol decomposition. Figure 7 shows a comparison of the matrix IR spectrum of CH_3CH_2SH heated to 1300 K with an authentic room-temperature IR spectra for H_2S (green trace). The absorption at 1179 cm^{-1} in the heated CH_3CH_2SH spectrum is unmistakably from the ν_2 vibrational mode in H_2S. Vibrational mode ν_3 = 2635 cm^{-1} was also observed for H_2S.

4. DISCUSSION. DECOMPOSITION MECHANISM OF ETHANETHIOL

These experiments have enabled us to identify the initial thermal decomposition products of ethanethiol. Using the high-temperature microtubular reactor, we have shown that ethanethiol thermally cracks into the three distinct pathways depicted in Scheme 1. To our knowledge, this work is the first to detect reactive intermediates in the thermal decompositions of ethanethiol. The three pathways found experimentally in this work agree well with the theoretical findings of Baldridge et al.[10] Additionally, the three decomposition channels proposed here are analogous to the currently accepted decomposition mechanisms for ethanol, which has been studied in great detail both experimentally and theoretically.[50,51]

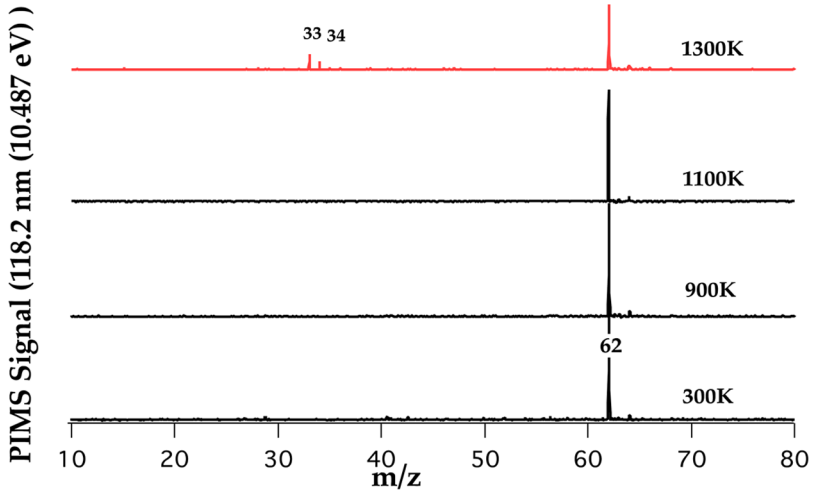

Figure 2. PIMS spectra of the decomposition products of ethanethiol in a high-temperature microtubular reactor.

DOI: 10.1021/acs.jpca.7b02629
J. Phys. Chem. A 2017, 121, 4953−4960

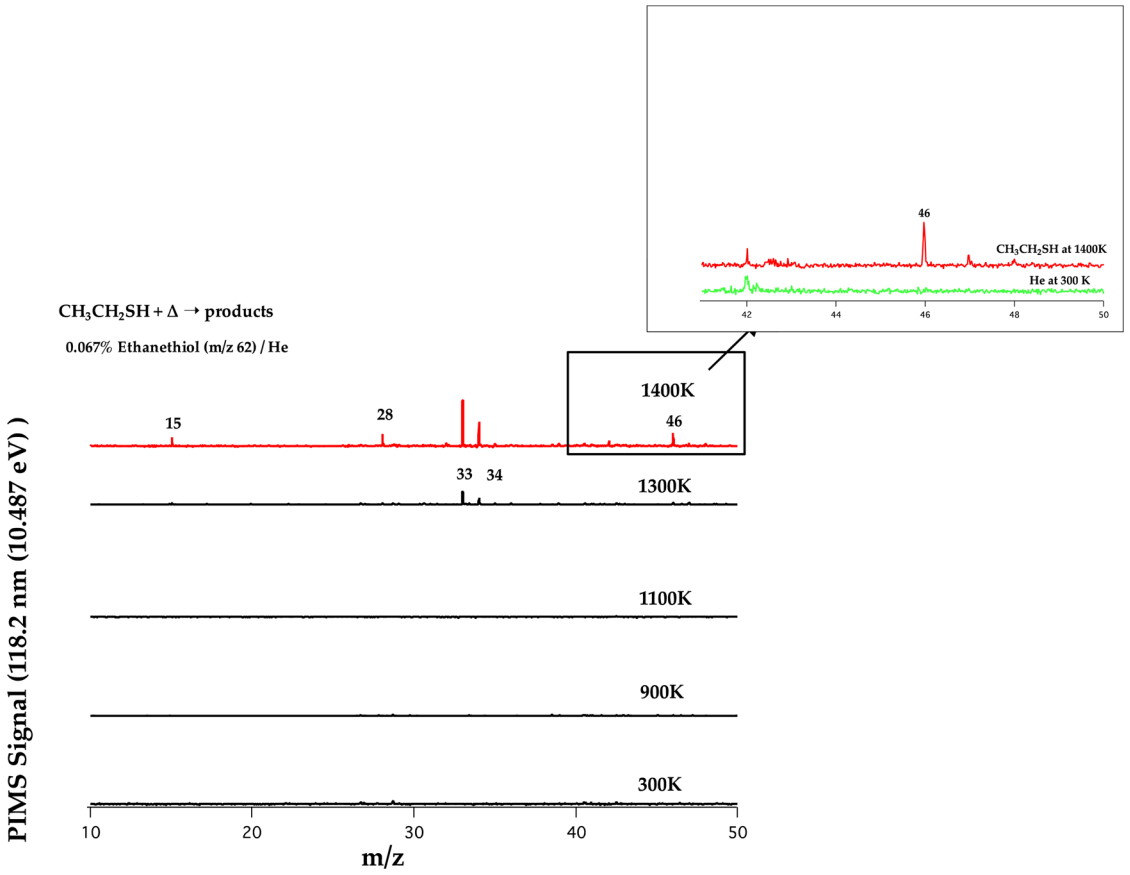

Figure 3. PIMS spectra for appearance of decomposition products from ethanethiol as the temperature of the microreactor is increased to 1400 K. The inset provides a more detailed view of the m/z 46 region.

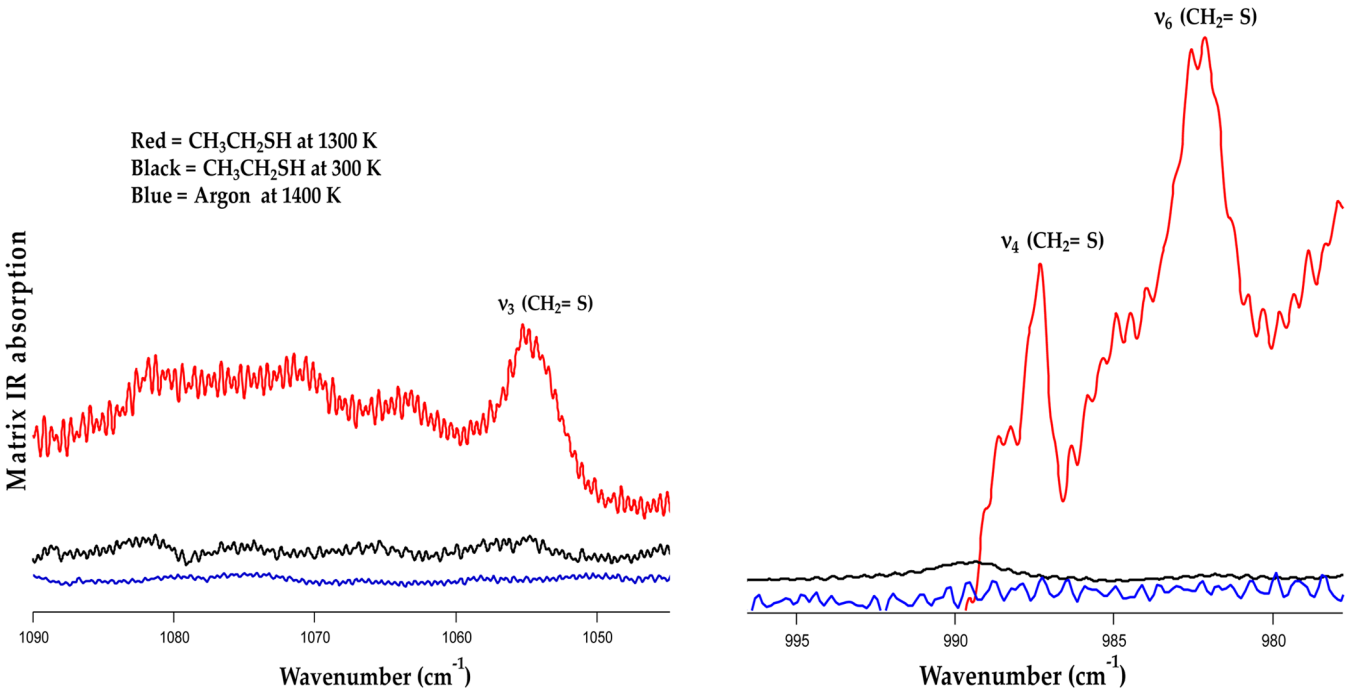

Figure 4. Matrix IR absorption spectra demonstrating the presence of thioformaldehyde (CH_2SH) following the pyrolysis of ethanethiol in a pulsed reactor (0.01% CH_3CH_2SH/Ar). The blue trace is that of the buffer gas Ar at 1400 K; the black and red traces are CH_3CH_2SH at room temperature and 1300 K, respectively. The known bands ν_6 = 982 cm^{-1}, ν_4 = 988 cm^{-1}, and ν_3 = 1055 cm^{-1} of CH_2SH are assigned.

The pathways for formation of CH_3CH_2 + SH (Scheme 1a) and CH_3 + $H_2C{=}S$ + H (Scheme 1b) are from the bond cleavages of C—S (73.6 ± 0.5 kcal mol^{-1}) and C—C (82.5 ± 2.2 kcal mol^{-1}), respectively. Although it has been shown at a range

DOI: 10.1021/acs.jpca.7b02629
J. Phys. Chem. A 2017, 121, 4953−4960

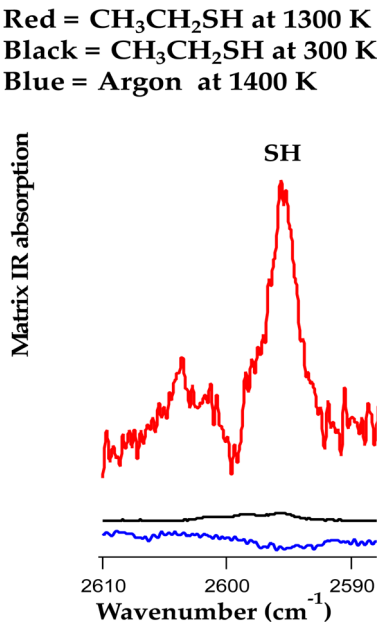

Figure 5. Matrix IR absorption spectra demonstrating the presence of the sulfanyl radical (SH) resulting from the thermal cracking of ethanethiol in a pulsed reactor (0.01% CH_3CH_2SH/Ar). The blue trace is that of the buffer gas Ar at 1400 K; the black and red traces are CH_3CH_2SH at room temperature and 1300 K, respectively. The single vibrational mode of SH has been assigned at 2595 cm^{-1}.

of pressures and temperatures within the microtubular reactor that the effective residence time is on the order of tens of microseconds, we expect that the lifetime of the product CH_3CH_2 radical is too short for observation and rapidly decomposes in the SiC reactor into ethylene and a hydrogen atom, $H_2C{=}CH_2$ + H.[50] The thioformaldhyde (Scheme 1b) observed in both PIMS and IR experiments results from the isomerization of the CH_2SH radical upon the C—C bond rupture ($CH_2SH \rightarrow H_2C{=}S + H$). This analogous isomerization ($CH_2OH \rightarrow H_2C{=}O$) is also observed in the thermal cracking of ethanol.[50]

The pathway for formation of $H_2C{=}CH_2 + H_2S$ (Scheme 1c) proceeds through an intramolecular elimination of ethanethiol.

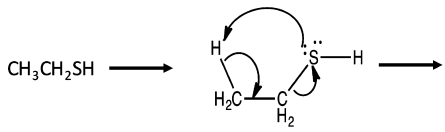

(4)

The barrier of formation for CH_2CH_2 and H_2S via the intramolecular pathway (4) is 75.9 kcal/mol, which is ≈2 kcal/mol higher than the measured C—S bond enthalpy.[10] The intramolecular pathway is also the most thermodynamically favorable pathway. This unimolecular intramolecular pathway (4) has been observed experimentally and theoretically in ethanol and found to have a similar barrier to decomposition of 75.9 kcal/mol.[44] The shock tube and experimental study by Park et al.[51] determined this product channel to be the dominant channel below 10 atm for ethanol in the temperature range 700–2500 K. A second combined shock tube and theoretical study by Sivaramakrishnan et al.[50] also found the intramolecular channel to be a primary pathway for the unimolecular decomposition of ethanol.

As hydrogen radicals in reactions a and b in Scheme 1 and the methyl radical in the Scheme 1b reaction are produced, discussion must be given to the possibility of bimolecular reactions involving these radicals with ethanethiol, specifically with reference to the intramolecular pathway. An advantage of the microtubular reactor used in our work is the short residence

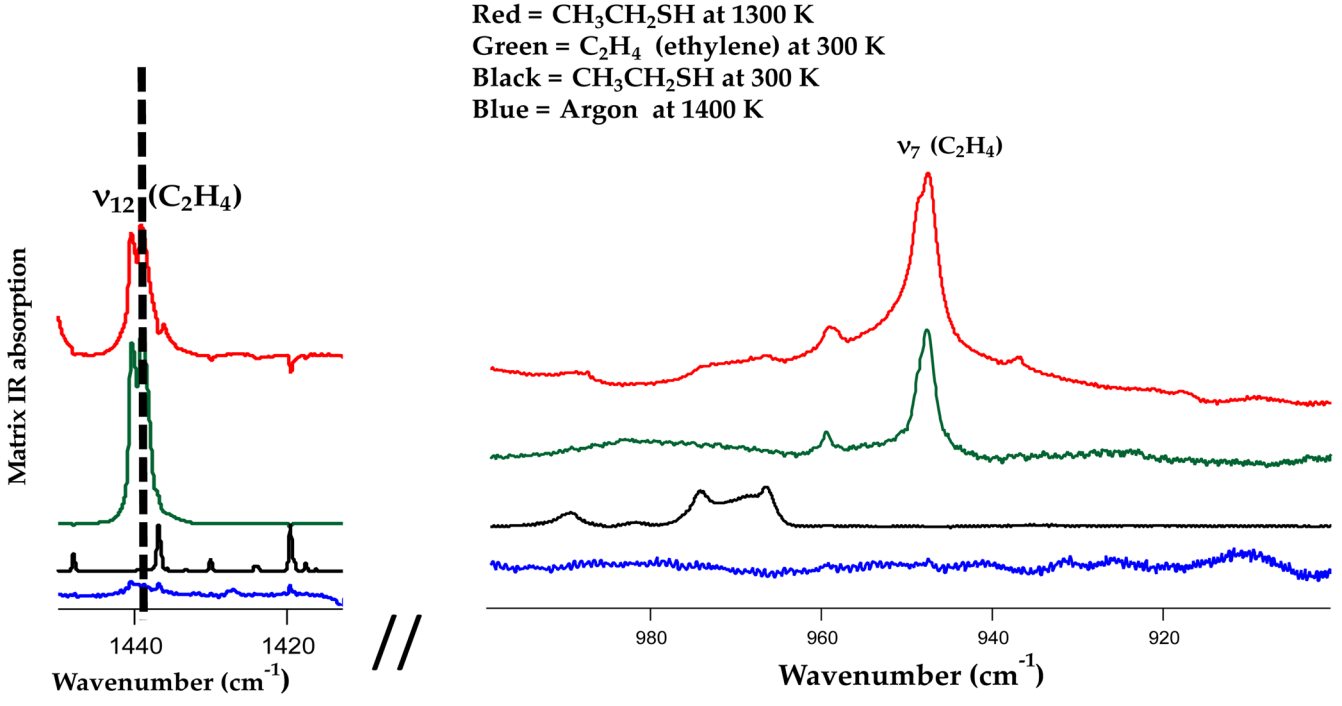

Figure 6. Matrix IR absorption spectra demonstrating the presence of ethylene ($H_2C{=}CH_2$) following the thermal cracking of ethanethiol in a pulsed reactor (0.01% CH_3CH_2SH/Ar). The blue trace is that of the buffer gas Ar at 1400 K, the black trace is CH_3CH_2SH at room temperature, the green trace is a spectrum of pure ethylene at 300 K, and the red trace results from heating CH_3CH_2SH to 1300 K. The IR features at 1439 and 947 cm^{-1} in the spectrum at 1300 K clearly belong to ν_{12} and ν_7 of ethylene.

DOI: 10.1021/acs.jpca.7b02629
J. Phys. Chem. A 2017, 121, 4953–4960

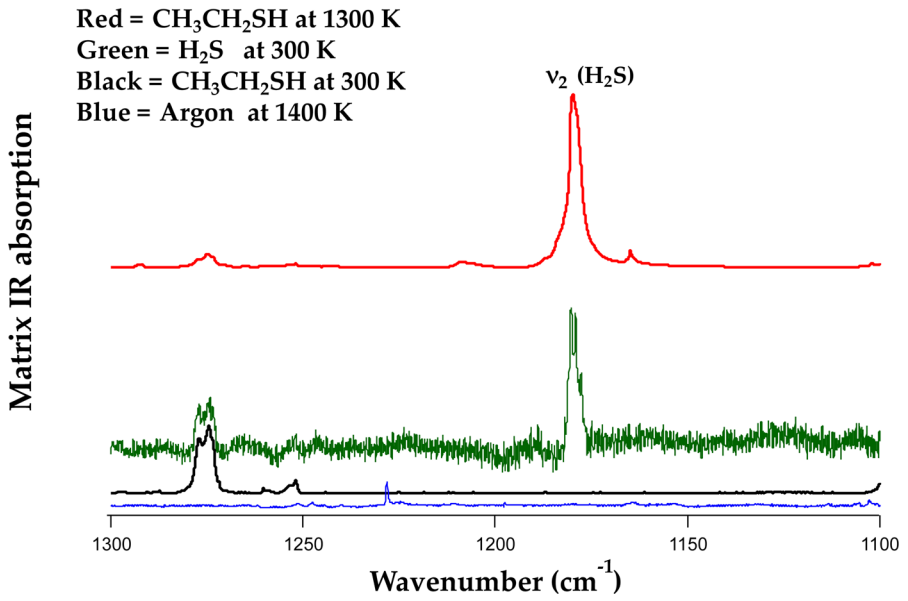

Figure 7. Matrix IR absorption spectra demonstrating the presence of hydrogen sulfide (H_2S) following the pyrolysis of ethanethiol in a pulsed reactor (0.01% CH_3CH_2SH/Ar). The blue trace is that of the buffer gas Ar at 1400 K, the black trace CH_3CH_2SH at room temperature, the green trace is a spectrum of pure H_2S at 300 K, and the red trace is the spectrum resulting from heating CH_3CH_2SH to 1300 K. The IR absorption at 1179 cm^{-1} in the 1300 K spectrum is confidently assigned to ν_2 of H_2S.

times, which help to minimize rapid secondary radical reactions. It has been shown by both experience and extensive simulation that the effective residence time in the microtubular reactor is on the order 50−100 μs.[27,52] The possible H radical reactions with ethanethiol and respective second-order rate constants reported by Zhang et al.[53] are as follows:

H abstraction from CH_3

$$CH_3CH_2SH + H \rightarrow CH_2CH_2SH + H_2$$
$$k(1400\ K) = 6.31 \times 10^{-13}\ cm^3\ molecules^{-1}\ s^{-1} \quad (5)$$

H abstraction from CH_2

$$CH_3CH_2SH + H \rightarrow CH_3CHSH + H_2$$
$$k(1400\ K) = 6.35 \times 10^{-12}\ cm^3\ molecules^{-1}\ s^{-1} \quad (6)$$

H abstraction from SH

$$CH_3CH_2SH + H \rightarrow CH_3CH_2S + H_2$$
$$k(1400\ K) = 6.30 \times 10^{-11}\ cm^3\ molecules^{-1}\ s^{-1} \quad (7)$$

substitution channel

$$CH_3CH_2SH + H \rightarrow CH_3CH_2 + H_2S$$
$$k(1400\ K) = 5.37 \times 10^{-11}\ cm^3\ molecules^{-1}\ s^{-1} \quad (8)$$

In the study by Guan et al.[27] the more rapid radical/radical reaction of $CH_3 + HCO \rightarrow CH_4 + CO$ ($k = 2 \times 10^{-10}$ cm^3 $molecules^{-1}$ s^{-1}) was studied in the microtubular reactor during the pyrolysis of acetaldehyde. It was determined that if the initial reactant concentration was less than 0.1%, then the half-life of radicals would be approximately 200 μs between 1200 and 1300 K. Since the effective reaction residence time is much shorter than this in the microtubular reactor, it is expected that even at elevated temperatures, if the initial concentration of the reactant is kept small, secondary reactions are minimized if not excluded all together. The radical reaction studied in Guan et al. is an order of magnitude faster than the most rapid of the possible bimolecular reactions of the H atom with ethanethiol (8). Although it is still possible that a small fraction of products $H_2C{=}CH_2$ and H_2S could result from the bimolecular substitution channel (8), it is much more likely based on energetics and the short residence time of the microtubular reactor that the proposed intramolecular elimination channel (4) is the major source of $H_2C{=}CH_2$ and H_2S in this study.

In addition to the bimolecular channels of CH_3CH_2SH with H atoms, we have also considered the reactions of the methyl radicals with ethanethiol. There are five likely reactions of the methyl radical with ethanethiol. Three of the five involve a hydrogen abstraction by the methyl radical from the CH_3, CH_2, or SH groups of ethanethiol. In each of these abstraction reactions methane, CH_4, is the product. Although the ionization energy of CH_4 (IE = 12.618 ± 0.004 eV)[54] is above the 10.487 eV of our VUV laser, it is very straightforward to detect CH_4 using IR spectroscopy. A pure sample of methane was deposited at room temperature in the matrix for comparison with the heated ethanethiol spectra. Methane was not observed in any of the spectra generated from the thermal cracking of ethanethiol. The lack of CH_4 in the matrix experiments allows us to confidently eliminate all three hydrogen abstraction reactions by the methyl radical. The remaining two potential bimolecular channels involving the methyl radical are a substitution analogous to (8) and a second substitution reaction.

substitution channel

$$CH_3CH_2SH + CH_3 \rightarrow H_3C{-}SH + CH_3CH_2 \quad (9)$$

substitution channel

$$CH_3CH_2SH + CH_3 \rightarrow H_3C{-}S{-}CH_2{-}CH_3 + H \quad (10)$$

The products methanethiol, $H_3C{-}SH$ (IE = 9.446 ± 0.010),[55] in reaction 9 and methyl ethyl sulfide, $H_3C{-}S{-}CH_2{-}CH_3$ (IE = 8.54 ± 0.1),[56] in reaction 10, if present, would have been detected in both PIMS and matrix IR experiments. The PIMS spectra of heated ethanethiol revealed no product peaks at m/z 48 or 76,

DOI: 10.1021/acs.jpca.7b02629
J. Phys. Chem. A 2017, 121, 4953−4960

corresponding to methanethiol and methyl ethyl sulfide, respectively. Additionally, no vibrational modes were observed for either species in the IR. Specifically, intense vibrational modes for methanethiol (ν_1 = 3015 cm^{-1}, ν_6 = 1072 cm^{-1}, and ν_8 = 710 cm^{-1})[57] and methyl ethyl sulfide (ν_{19} = 2976 cm^{-1}, ν_{22} = 1457 cm^{-1}, ν_7 = 1446 cm^{-1}, and ν_{11} = 1269 cm^{-1})[58] were all absent in the IR. The lack of spectral signatures in both experimental techniques is convincing evidence that the substitution reactions 9 and 10 are not taking place during the thermal cracking of ethanethiol. All efforts to detect the methyl radical in the matrix failed. Previous studies have shown that it is difficult to detect the methyl radical as a pyrolysis product using matrix isolation spectroscopy.[22,24,59]

5. CONCLUSION

We have studied the thermal decomposition of ethanethiol in a pulsed microtubular reactor at short residence times (50−100 μs). The reactions were monitored with matrix isolation spectroscopy and VUV photoionization mass spectrometry. The experimental data collected are explained by the unimolecular decomposition of ethanethiol to its pyrolysis products. The thermal decomposition of ethanethiol produces three unique product channels: (CH_3CH_2 + SH), (CH_3 + H_2C=S + H), and (H_2C=CH_2 + H_2S). No evidence was found for bimolecular chemistry.

AUTHOR INFORMATION

Corresponding Author

*E-mail: avasiliou@middlebury.edu. Phone: 802-443-5517. (A. K. Vasiliou)

ORCID

AnGayle K. Vasiliou: 0000-0001-5963-4014

Present Address

‡Department of Chemistry, University of Washington, Seattle, WA 98195-1700 United States.

Notes

The authors declare no competing financial interest.

ACKNOWLEDGMENTS

This research was supported by grants provided by the National Science Foundation (CHE-1566282) and by donors of the American Chemical Society Petroleum Research Fund. The research reported in this publication was supported by the Institutional Development Award (IDeA) program from the National Institute of General Medical Sciences of the National Institutes of Health under grant no. P20GM103449. Its content is solely the responsibility of the authors and do not necessarily represent the official views of NIGMS or NIH.

REFERENCES

(1) Sabatier, S.; Mailhe, C. R. General Methods for Direct Preparation of Mercaptans by Catalysis Starting with the Alcohols. *C.R. Chim.* **1910**, *150*, 1217−1221.

(2) Sehon, A. H.; Darwent, B. deB The Thermal Decomposition of Mercaptans. *J. Am. Chem. Soc.* **1954**, *76*, 4806−4810.

(3) Trenner, N. R.; Taylor, H. A. The Thermal Decomposition of Ethyl Mercaptan and Ethyl Sulphide. *J. Chem. Phys.* **1933**, *1*, 77−88.

(4) Boivin, J. L.; MacDonald, R. Pyrolysis of Ethyl Mercaptan. *Can. J. Chem.* **1955**, *33*, 439−443.

(5) Bamkole, T. O. The Pyrolysis of Alkanethiols. Part 1. Kinetics of the Pyrolysis of Butane-1-Thiol, Butane-2-Thiol, and 2-Methylpropane-2-Thiol. *J. Chem. Soc., Perkin Trans. 2* **1977**, *4*, 439−443.

(6) Malisoff, W. M.; Marks, E. M. Thermal Behavior of Sulfur Compounds in Hydrocarbon Solvents I—Aliphatic Mercaptans. *Ind. Eng. Chem.* **1931**, *23*, 1114−1120.

(7) Tsang, W. Thermal Decomposition of Some Tert-Butyl Compounds at Elevated Temperatures. *J. Chem. Phys.* **1964**, *40*, 1498−1505.

(8) Thompson, C. J.; Meyer, R. A.; Ball, J. S. Thermal Decomposition of Sulfur Compounds. I. 2-Methyl-2-Propanethiol. *J. Am. Chem. Soc.* **1952**, *74*, 3284−3287.

(9) Thompson, C. J.; Meyer, R. A.; Ball, J. S. Thermal Decomposition of Sulfur Compounds. II. 1-Pentanethiol. *J. Am. Chem. Soc.* **1952**, *74*, 3287−3289.

(10) Baldridge, K. K.; Gordon, M. S.; Johnson, D. E. Thermal Decomposition of Methanethiol and Ethanethiol. *J. Phys. Chem.* **1987**, *91*, 4145−4155.

(11) Pedley, J. *Thermochemical Data and Structures of Organic Compounds*; Thermodynamics Research Center (TRC): College Station, TX, 1994; Vol. *1*, pp 252−253.

(12) McCullough, J. P.; Hubbard, W. N.; Frow, F. R.; Hossenlopp, I. A.; Waddington, G. Ethanethiol and 2-Thiapropane: Heats of Formation and Isomerization; The Chemical Thermodynamic Properties from 0 to 1000 K. *J. Am. Chem. Soc.* **1957**, *79*, 561−566.

(13) Luo, Y.-R. *Handbook of Bond Dissociation Energies in Organic Compounds*; CRC Press: Boca Raton, FL, 2002.

(14) Wilson, S. H. S. On the near Ultraviolet Photodissociation of Hydrogen Sulphide. *Mol. Phys.* **1996**, *88*, 841−858.

(15) Jochnowitz, E. B.; Zhang, X.; Nimlos, M. R.; Varner, M. E.; Stanton, J. F.; Ellison, G. B. Propargyl Radical: Ab Initio Anharmonic Modes and the Polarized Infrared Absorption Spectra of Matrix-Isolated $HCCCH_2$. *J. Phys. Chem. A* **2005**, *109*, 3812−3821.

(16) Kato, S.; Ellison, G. B.; Bierbaum, V. M.; Blanksby, S. J. Base-Induced Decomposition of Alkyl Hydroperoxides in the Gas Phase. Part 3. Kinetics and Dynamics in HO- + CH_3OOH, C_2H_5OOH, and Tert-C_4H_9OOH Reactions. *J. Phys. Chem. A* **2008**, *112*, 9516−9525.

(17) Ormond, T. K.; Hemberger, P.; Troy, T. P.; Ahmed, M.; Stanton, J. F.; Ellison, G. B. The Ionisation Energy of Cyclopentadienone: A Photoelectron−photoion Coincidence Study. *Mol. Phys.* **2015**, *113*, 2350−2358.

(18) Robichaud, D. J.; Scheer, A. M.; Mukarakate, C.; Ormond, T. K.; Buckingham, G. T.; Ellison, G. B.; Nimlos, M. R. Unimolecular Thermal Decomposition of Dimethoxybenzenes. *J. Chem. Phys.* **2014**, *140*, 234302.

(19) Scheer, A. M.; Mukarakate, C.; Robichaud, D. J.; Nimlos, M. R.; Ellison, G. B. Thermal Decomposition Mechanisms of the Methoxyphenols: Formation of Phenol, Cyclopentadienone, Vinylacetylene, and Acetylene. *J. Phys. Chem. A* **2011**, *115*, 13381−13389.

(20) Buckingham, G. T.; Ormond, T. K.; Porterfield, J. P.; Hemberger, P.; Kostko, O.; Ahmed, M.; Robichaud, D. J.; Nimlos, M. R.; Daily, J. W.; Ellison, G. B. The Thermal Decomposition of the Benzyl Radical in a Heated Micro-Reactor. I. Experimental Findings. *J. Chem. Phys.* **2015**, *142*, 044307.

(21) Vasiliou, A.; Nimlos, M. R.; Daily, J. W.; Ellison, G. B. Thermal Decomposition of Furan Generates Propargyl Radicals. *J. Phys. Chem. A* **2009**, *113*, 8540−8547.

(22) Vasiliou, A. K.; Piech, K. M.; Reed, B.; Zhang, X.; Nimlos, M. R.; Ahmed, M.; Golan, A.; Kostko, O.; Osborn, D. L.; David, D. E.; et al. Thermal Decomposition of CH3CHO Studied by Matrix Infrared Spectroscopy and Photoionization Mass Spectroscopy. *J. Chem. Phys.* **2012**, *137*, 164308.

(23) Vasiliou, A. K.; Kim, J. H.; Ormond, T. K.; Piech, K. M.; Urness, K. N.; Scheer, A. M.; Robichaud, D. J.; Mukarakate, C.; Nimlos, M. R.; Daily, J. W.; et al. Biomass Pyrolysis: Thermal Decomposition Mechanisms of Furfural and Benzaldehyde. *J. Chem. Phys.* **2013**, *139*, 104310.

(24) Vasiliou, A.; Piech, K. M.; Zhang, X.; Nimlos, M. R.; Ahmed, M.; Golan, A.; Kostko, O.; Osborn, D. L.; Daily, J. W.; Stanton, J. F.; et al. The Products of the Thermal Decomposition of CH_3CHO. *J. Chem. Phys.* **2011**, *135*, 014306.

DOI: 10.1021/acs.jpca.7b02629
J. Phys. Chem. A 2017, 121, 4953−4960

(25) Prozument, K.; Park, G. B.; Shaver, R. G.; Vasiliou, A. K.; Oldham, J. M.; David, D. E.; Muenter, J. S.; Stanton, J. F.; Suits, A. G.; Ellison, G. B.; et al. Chirped-Pulse Millimeter-Wave Spectroscopy for Dynamics and Kinetics Studies of Pyrolysis Reactions. *Phys. Chem. Chem. Phys.* **2014**, *16*, 15739−15751.
(26) Chen, P.; Colson, S. D.; Chupka, W. A.; Berson, J. A. Flash Pyrolytic Production of Rotationally Cold Free Radicals in a Supersonic Jet. Resonant Multiphoton Spectrum of the $3p^2A_2''$.rarw. X^2A_2'' origin Band of Methyl. *J. Phys. Chem.* **1986**, *90*, 2319−2321.
(27) Guan, Q.; Urness, K. N.; Ormond, T. K.; David, D. E.; Barney Ellison, G.; Daily, J. W. The Properties of a Micro-Reactor for the Study of the Unimolecular Decomposition of Large Molecules. *Int. Rev. Phys. Chem.* **2014**, *33*, 447−487.
(28) Meyer, B. *Low Temperature Spectroscopy*; American Elsevier: New York, 1971.
(29) Norrish, R. G. W.; Porter, G. Chemical Reactions Produced by Very High Light Intensities. *Nature* **1949**, *164*, 658−658.
(30) Colussi, A. J.; Benson, S. W. The Very Low-Pressure Pyrolysis of Phenyl Methyl Sulfide and Benzyl Methyl Sulfide. The Enthalpy of Formation of the Methylthio and Phenylthio Radicals. *Int. J. Chem. Kinet.* **1977**, *9*, 295−306.
(31) Zheng, X.; Fisher, E. M.; Gouldin, F. C.; Zhu, L.; Bozzelli, J. W. Experimental and Computational Study of Diethyl Sulfide Pyrolysis and Mechanism. *Proc. Combust. Inst.* **2009**, *32*, 469−476.
(32) Zheng, X.; Fisher, E. M.; Gouldin, F. C.; Bozzelli, J. W. Pyrolysis and Oxidation of Ethyl Methyl Sulfide in a Flow Reactor. *Combust. Flame* **2011**, *158*, 1049−1058.
(33) Shum, L. G. S.; Benson, S. W. The Pyrolysis of Dimethyl Sulfide, Kinetics and Mechanism. *Int. J. Chem. Kinet.* **1985**, *17*, 749−761.
(34) Shum, L. G. S.; Benson, S. W. Iodine Catalyzed Pyrolysis of Dimethyl Sulfide. Heats of Formation of CH_3SCH_2I, the CH_3SCH_2 Radical, and the Pibond Energy in CH_2S. *Int. J. Chem. Kinet.* **1985**, *17*, 277−292.
(35) Brown, A. L.; Dayton, D. C.; Nimlos, M. R.; Daily, J. W. Design and Characterization of an Entrained Flow Reactor for the Study of Biomass Pyrolysis Chemistry at High Heating Rates. *Energy Fuels* **2001**, *15*, 1276−1285.
(36) Porterfield, J. P.; Nguyen, T. L.; Baraban, J. H.; Buckingham, G. T.; Troy, T. P.; Kostko, O.; Ahmed, M.; Stanton, J. F.; Daily, J. W.; Ellison, G. B. Isomerization and Fragmentation of Cyclohexanone in a Heated Micro-Reactor. *J. Phys. Chem. A* **2015**, *119*, 12635−12647.
(37) Choi, S.; Kang, T. Y.; Choi, K.-W.; Han, S.; Ahn, D.-S.; Baek, S. J.; Kim, S. K. Conformationally Specific Vacuum Ultraviolet Mass-Analyzed Threshold Ionization Spectroscopy of Alkanethiols: Structure and Ionization of Conformational Isomers of Ethanethiol, Isopropanethiol, 1-Propanethiol, Tert-Butanethiol, and 1-Butanethiol. *J. Phys. Chem. A* **2008**, *112*, 7191−7199.
(38) Hsu, C.-W.; Baldwin, D. P.; Liao, C.-L.; Ng, C. Y. Rotationally Resolved Nonresonant Two-photon Ionization of SH. *J. Chem. Phys.* **1994**, *100*, 8047−8054.
(39) Prest, H. F.; Tzeng, W.-B.; Brom, J. M., Jr.; Ng, C. Y. Molecular Beam Photoionization Study of H2S. *Int. J. Mass Spectrom. Ion Phys.* **1983**, *50*, 315−329.
(40) Berkowitz, J.; Ellison, G. B.; Gutman, D. Three Methods to Measure RH Bond Energies. *J. Phys. Chem.* **1994**, *98*, 2744−2765.
(41) Cool, T. A.; Wang, J.; Nakajima, K.; Taatjes, C. A.; Mcllroy, A. Photoionization Cross Sections for Reaction Intermediates in Hydrocarbon Combustion. *Int. J. Mass Spectrom.* **2005**, *247*, 18−27.
(42) Ruscic, B.; Berkowitz, J. Photoionization Mass Spectrometry of CH2S and HCS. *J. Chem. Phys.* **1993**, *98*, 2568−2579.
(43) Jacox, M. E.; Milligan, D. E. Matrix Isolation Study of the Infrared Spectrum of Thioformaldehyde. *J. Mol. Spectrosc.* **1975**, *58*, 142−157.
(44) Torres, M.; Safarik, I.; Clement, A.; Strausz, O. P. The Generation of Vibrational Spectrum of Matrix Isolated Thioformaldehyde and Dideuterothioformaldehyde. *Can. J. Chem.* **1982**, *60*, 1187−1191.
(45) Isoniemi, E.; Pettersson, M.; Khriachtchev, L.; Lundell, J.; Räsänen, M. Infrared Spectroscopy of H_2S and SH in Rare-Gas Matrixes. *J. Phys. Chem. A* **1999**, *103*, 679−685.
(46) Anderson, D. T.; Winn, J. S. Matrix Isolated HF: The High-Resolution Infrared Spectrum of a Cryogenically Solvated Hindered Rotor. *Chem. Phys.* **1994**, *189* (2), 171−178.
(47) Koga, K.; Takami, A.; Koda, S. IR Spectra of H_2S Isolated in Free-Standing Crystals of Kr and Xe. *Chem. Phys. Lett.* **1998**, *293*, 180−184.
(48) Lorenz, M.; Kraus, D.; Rasanen, M.; Bondybey, V. E. Photodissociation of Hydrogen Halides in Rare Gas Matrixes, and the Effect of Hydrogen Bonding. *J. Chem. Phys.* **2000**, *112*, 3803−3811.
(49) Pimentel, G. C.; Bulanin, M. O.; Thiel, M. V. Infrared Spectra of Ammonia Suspended in Solid Nitrogen. *J. Chem. Phys.* **1962**, *36*, 500−506.
(50) Sivaramakrishnan, R.; Su, M.-C.; Michael, J. V.; Klippenstein, S. J.; Harding, L. B.; Ruscic, B. Rate Constants for the Thermal Decomposition of Ethanol and Its Bimolecular Reactions with OH and D: Reflected Shock Tube and Theoretical Studies. *J. Phys. Chem. A* **2010**, *114*, 9425−9439.
(51) Park, J.; Zhu, R. S.; Lin, M. C. Thermal Decomposition of Ethanol. I. Ab Initio Molecular Orbital/Rice-Ramsperger-Kassel-Marcus Prediction of Rate Constant and Product Branching Ratios. *J. Chem. Phys.* **2002**, *117*, 3224−3231.
(52) Zhang, X.; Friderichsen, A. V.; Nandi, S.; Ellison, G. B.; David, D. E.; McKinnon, J. T.; Lindeman, T. G.; Dayton, D. C.; Nimlos, M. R. Intense, Hyperthermal Source of Organic Radicals for Matrix-Isolation Spectroscopy. *Rev. Sci. Instrum.* **2003**, *74*, 3077−3086.
(53) Zhang, Q.; Wang, H.; Sun, T.; Wang, W. A Theoretical Investigation for the Reaction of CH_3CH_2SH with Atomic H: Mechanism and Kinetics Properties. *Chem. Phys.* **2006**, *324*, 298−306.
(54) Signorell, R.; Merkt, F. The First Rotationally Resolved Spectrum of CH_4^+. *J. Chem. Phys.* **1999**, *110*, 2309−2311.
(55) Nourbakhsh, S.; Norwood, K.; Yin, H.-M.; Liao, C.-L.; Ng, C. Y. Vacuum Ultraviolet Photodissociation and Photoionization Studies of CH_3SH and SH. *J. Chem. Phys.* **1991**, *95*, 946−954.
(56) Keyes, B. G.; Harrison, A. G. Fragmentation of Aliphatic Sulfur Compounds by Electron Impact. *J. Am. Chem. Soc.* **1968**, *90*, 5671−5676.
(57) May, I. W.; Pace, E. L. Vibrational Spectra of Methanethiol. *Spectrochim. Acta. A. Mol. Biomol. Spectrosc.* **1968**, *24*, 1605−1615.
(58) Durig, J. R.; Rollins, M. S.; Phan, H. V. Conformational Stability, Barriers to Internal Rotation, Ab Initio Calculations and Vibrational Assignment of Ethyl Methyl Sulfide. *J. Mol. Struct.* **1991**, *263*, 95−122.
(59) Jacox, M. E. Matrix Isolation Study of the Infrared Spectrum and Structure of the CH_3 Free Radical. *J. Mol. Spectrosc.* **1977**, *66*, 272−287.

DOI: 10.1021/acs.jpca.7b02629
J. Phys. Chem. A 2017, 121, 4953−4960